Behavioral/System/Cognitive
Senior editor: David Fitzpatrick

Influence of contrast on the spatial frequency tuning of neuronal populations in the cat visual thalamus

Chong Weng[1*], Jianzhong Jin[1*], Chun-I Yeh[2] & Jose-Manuel Alonso[1]

[1]Department of Biological Sciences
State University of New York – State College of Optometry
33 West 42nd Street
New York, NY 10036

[2]Center for Neural Science
New York University
4 Washington Place
New York, NY 10003-6603

*These two authors contributed equally to this work.

Correspondence should be addressed to:
Jose-Manuel Alonso
Department of Biological Sciences
State University of New York – State College of Optometry
33 West 42nd Street
New York, NY 10036, USA
Phone: (212) 938-5573
Fax: (212) 938-5796
Email: jalonso@sunyopt.edu

Abbreviated title: Contrast-dependent spatial frequency tuning in LGN
Number of figures: 6
Number of pages: 26
Number of words in Abstract/Introduction/Discussion: 240/380/771

Keywords: LGN, striate cortex, visual cortex, receptive field, neural coding, thalamocortical

Acknowledgements: This work was supported by NIH (EY 05253) and the Research Foundation at State University of New York. We thank Nadia Gamez Gomez and Javier Cubo Villalba for helping in the development of analysis software.

Abstract

While spatial frequency tuning was traditionally thought to be independent of contrast, recent studies have demonstrated clear contrast-dependent changes in both thalamus and cortex. To investigate the consequences of these changes at the level of neuronal populations, we made simultaneous recordings from neighboring cat geniculate cells and measured spatial frequency tuning of each individual neurons and the neuronal populations at different contrasts. Increasing the contrast not only broadened the spatial frequency tuning of the individual cells, but also caused shifts in their optimal spatial frequencies that could be either towards lower or higher frequencies (peak shifts). Interestingly, these peak shifts were not random but depended on the optimal spatial frequency of the cell: cells with low optimal spatial frequencies (< 0.4 c/d) shifted their peaks towards lower frequencies and those with high optimal spatial frequencies (> 0.5 c/d) shifted towards higher frequencies. The value of peak shift was significantly correlated with the optimal spatial frequency of the cell measured at high contrast in our data and similar unreported correlations were found when we re-analyzed the thalamic and cortical data from previous studies. Our results indicate that increasing the contrast has a major effect on the spatial frequency tuning of cell populations within LGN and that this population tuning is broadened by two different mechanisms: tuning-broadening of single-cell spatial-frequency bandwidth and tuning-stretching of the cell-population bandwidth, the latter one caused by peak shifts in opposite directions of the spatial frequency spectrum.

Introduction

While contrast can greatly influence the magnitude of neuronal responses at nearly all stages of visual processing, single neuron investigations demonstrated that preferred spatial frequency tuning of cortical cells are relatively independent of stimulus contrast (Movshon et al., 1978; Albrecht and Hamilton, 1982; Li and Creutzfeldt, 1984; Bradley et al., 1987; Skottun et al., 1987; Sclar et al., 1990). Models where responses are normalized over contrast to maintain contrast-invariant spatial frequency tuning curves have been proposed to explain these results (Ohzawa et al., 1985; Heeger, 1992). However, recent studies in both primate primary visual cortex (V1) and cat lateral geniculate nucleus (LGN) have challenged this point of view (Sceniak et al., 2002; Nolt et al., 2004). In particular, it has been shown that the spatial frequency tunings of individual thalamic and cortical neurons are not totally independent of contrast: increasing the contrast clearly increased the bandwidth of spatial frequency tuning of these neurons.

The consequences of these contrast-dependent changes of spatial frequency tunings at the level of neuronal populations remain to be determined. Here, we made simultaneous recordings from neighboring neurons with overlapping receptive fields in the cat LGN and measured the spatial frequency tuning of each individual neuron and the neuronal populations. On average, the spatial frequency bandwidth was broader at high contrast than low contrast when measured both directly from the response of individual cells (29% broader) and from the normalized summed-response of neuronal populations (36% broader). Increasing contrast also produced a shift in the peak of the spatial frequency tuning of the geniculate cells (towards higher frequencies in band-pass cells

and lower frequencies in low-pass cells). And this peak shift was significantly correlated with the optimal spatial frequency of the cell. When we re-analyzed the thalamic and cortical data from previous studies (Sceniak et al., 2002; Nolt et al., 2004), we found similar unreported correlation in both. Our results indicate that increasing contrast not only broadens the spatial frequency tuning at the level of single neurons (by making each tuning curve wider), but also at the level of neuronal populations (by stretching the peak of the spatial frequency tuning in different directions depending on the spatial frequency peak of the cell). Preliminary results were previously published in abstract form (Jin et al., 2004; Weng et al., 2007).

Materials and Methods

Surgery and preparation

Cats were initially anesthetized with Ketamine (10 mg/kg, intramuscular) followed by thiopental sodium (20 mg/kg, intravenous, supplemented as needed during surgery; and at a continuous rate of 1-2 mg/kg/hr, intravenous, during recording). Lidocaine was administered topically or injected subcutaneously at all incisions or points of pain and pressure. The animal was then intubated and placed in a stereotaxic apparatus. We monitored the following vital signs: electrocardiogram, electroencephalogram, oxygen in blood (measured by pulse oximetry), expired carbon dioxide, heart rate, blood pressure (measured with a pressure cuff), hydration (urinary specific gravity) and rectal temperature. A craniotomy and duratomy were made to introduce recording electrodes into LGN (anterior: 5.5; lateral 10.5). Animals were paralyzed with Atracurium Besylate (0.6-1 mg/kg/hr, intravenous) to minimize eye movements and artificially ventilated to keep the expired CO_2 between 28-33 mmHg. Pupils were dilated with atropine sulfate (1%) and the nictitating membranes were retracted with Neo-Synephrine (10%). High-permeability contact lenses were used to refract the animal properly and protect the eyes from drying. The optic disk and the area centralis were projected onto a tangent screen located 114 cm from the cat (Pettigrew et al., 1979). All surgical and experimental procedures were performed in accordance with United States Department of Agriculture (USDA) guidelines and were approved by the Institutional Animal Care and Use Committee (IACUC) at the State University of New York, State College of Optometry.

Electrophysiological recordings and data acquisition

A matrix of seven independently moveable electrodes arranged circularly was introduced into the LGN (Eckhorn and Thomas, 1993). The electrodes were sharp and thin (80 μm rod) and had impedances of 3-6 MΩ (System Eckhorn Thomas Recordings, Marburg, Germany). A glass guide tube with an inner diameter of about 300 μm at the tip was attached to the shaft probe of the multi-electrode to reduce the inter-electrode distances to approximately 80-300 μm. The matrix of electrodes was then lowered into the brain, leaving the tip of the guide tube ~3 mm above the LGN. Each electrode was moved independently within the LGN and positioned within layer A. The angle of the multi-electrode was adjusted precisely for each experiment (~25-30˚ anterior-posterior; ~2-5˚ lateral-central) to simultaneously record from cells with spatially overlapping receptive fields. All cells were recorded within 5-10 degrees of the area centralis. Recorded voltage signals from all seven electrodes were conventionally amplified, filtered, and passed to a computer running the Discovery software package (Datawave System, Longmont, CO). For each cell, spike waveforms were identified initially during the experiment and verified carefully off-line by spike sorting analysis (Datawave System, Longmont, CO). Visual stimuli were generated with an AT-vista graphics card (Truevision, Indianapolis, IN) and shown on a 20-inch monitor (Nokia 445Xpro, Salo, Finland; frame rate: 128 Hz).

Spatial frequency tuning

The spatial frequency tuning of all LGN cells was measured with full-screen sinusoidal drifting gratings at two different contrasts (high: 98% and low: 22%). At each contrast, there were 10 trials of 10 different spatial frequencies with a range of 0.07-4.44 cycle/degree. Within each trial, grating of each spatial frequency was presented for 4

cycles with temporal frequency of 2 Hz. The mean firing rates were measured and then fitted with Gaussian functions, which generated very accurate representations of neuronal response, with goodness of fitting values of 0.96 ± 0.04 for high contrast data and 0.95 ± 0.04 for low contrast data. And the Gaussian fitted curve was then normalized for better comparison between low and high contrasts. From the fitted and normalized Gaussian curves, we obtained two parameters: spatial frequency peak (SF-Peak) and spatial frequency half-bandwidth (SF-Bandwidth). The SF-Peak was defined as the spatial frequency value that elicited the maximal response. The SF-Bandwidth was defined as $\log_2$ (SF-High cutoff/SF-Peak), where SF-High cutoff is the spatial frequency that produced half of the maximum response (on the right side of the Gaussian).

Receptive field mapping

Receptive fields were mapped with white noise by reverse correlation, which consisted of 16x16 checkerboards of black and white pixels (15.5 ms/checkerboard; 0.9 degrees/pixel) (Yeh et al., 2003). The receptive fields mapped by reverse correlation were represented as contour plots smoothed with a cubic spline, with each contour line showing from center to periphery 100 to 20% of the maximum response (Matlab, The MathWorks, Natick, MA). For clarity, only the most external 20% contour lines are represented when showing superimposed receptive fields. On-center receptive fields are shown as continuous lines and off-center receptive fields as discontinuous lines.

Classification of cells

All geniculate cells recorded from layers A were classified as X or Y based on the linearity of spatial summation, measured with contrast reverse sinusoidal gratings (Enroth-Cugell and Robson, 1966; Shapley and Hochstein, 1975; Hochstein and Shapley, 1976). We used at least two different spatial frequencies that were higher than the optimal spatial frequency, usually 0.55 cycle/deg and 1.1 cycle/deg. Because some Y cells can generate linear responses when tested with very low spatial frequencies, high spatial frequencies were used to unambiguously classify groups of X and Y geniculate cells that were simultaneously recorded (Hochstein and Shapley, 1976; So and Shapley, 1979). Each spatial frequency was tested at eight different phases. The gratings were presented at 0.4 Hz and repeated at least 8 times at each spatial phase. The Y/X identification was always made from the response to the highest spatial frequency that generated a significant response ($\geqslant$ 5 spikes / 50 ms bin). Cells that responded poorly ($<$ 5 spikes / 50 ms bin) were labeled as unclassified. In this study, we only included X and Y cells recorded in layer A.

Results

Simultaneous recordings from several neighboring geniculate cells were made by using a matrix of seven independently movable electrodes (Eckhorn and Thomas, 1993). These electrodes were positioned very close to each other (80-300 microns apart) within layer A of cat LGN to record from neighboring neurons with overlapping receptive fields (average ~7 cells per population). Figure 1 shows a representative population of 7 geniculate cells that were simultaneously recorded. The receptive field centers, mapped with white noise by reverse correlation at high contrast (98%), are shown as contour plots at the center. For clarity, only the most external 20% contour lines are represented when showing superimposed receptive fields (on-center cells are shown in continuous lines and off-center cells in discontinuous lines, see Methods for details). The spatial frequency tuning curves, measured with drifting sinusoidal gratings at high and low contrasts (98% and 22%) and fitted with Gaussian functions, are shown at the periphery. We obtained two parameters from the fitted Gaussian curves: spatial frequency peak (SF-Peak) and half-bandwidth (SF-Bandwidth). SF-Peak was defined as the spatial frequency value that elicited the maximal response. And SF-Bandwidth was calculated as the log ratio in octaves ($\log_2$ (SF-High cutoff/SF-Peak)), where SF-High cutoff was the spatial frequency that produced half of the maximum response on the right side of the Gaussian curve. As the stimulus contrast increased, the SF-Bandwidths became broader in all the cells and the SF-peaks shifted towards lower (Cells 1~4) or higher (Cells 6~7) spatial frequencies.

Most cells demonstrated a significant SF-Bandwidth broadening as contrast increased (107 of the 132 cells studied). On average, the SF-bandwidth of all the 132 cells became 29% broader at high contrast than low contrast (1.18 vs. 0.91 octaves, $p <$

0.001, Wilcoxon test, Fig. 2A). This result is in agreement with previous studies in cat LGN and primate V1 (Sceniak et al., 2002; Nolt et al., 2004). Moreover, the mean SF-Bandwidth ratios (SF-Bandwidth at high contrast/SF-Bandwidth at low contrast) for X cells (1.40) and Y cells (1.43) were not significantly different ($p > 0.05$, Wilcoxon test, Fig. 2B-C). When we normalized, summed and then averaged the spatial frequency tuning curve of each individual cell within each cell population, we found that the SF-bandwidth measured from the summed-response of neuronal populations also increased with contrast by 36% (1.25 vs. 0.92 octaves, $p < 0.001$, Wilcoxon test).

When we compared the SF-Peak at different contrasts cell by cell, there seemed to be no contrast-dependent change in SF-Peak on average ($p > 0.05$, Wilcoxon test, Fig. 3A). The SF-Peak ratios (SF-Peak at high contrast/SF-Peak at low contrast) of X cells (0.95) and Y cells (1.04) were also very similar ($p > 0.05$, Wilcoxon test, Fig. 3B-C). However, increasing the contrast did create shifts in the optimal spatial frequency of the individual cells that could be either towards lower or higher frequencies (peak shifts). Interestingly, the peak shifts were not random but depended on the SF-Peak of the cell: the value of peak shift was significantly correlated with the optimal spatial frequency of the cell measured at high contrast (All cells: $r = 0.57$, $p < 0.001$; X cells: $r = 0.72$, $p < 0.001$; Y cells: $r = 0.43$, $p<0.001$, Fig. 4A). Furthermore, we divided all the LGN cells into 6 groups based on their SF-Peaks at high contrast and then averaged all the cells within each group (Figure 4B). Cells with low optimal spatial frequencies (< 0.4 c/d) shifted their peaks towards lower frequencies (average shift = -0.05 c/d, $p < 0.001$, Wilcoxon test) and those with high optimal spatial frequencies (> 0.5 c/d) shifted towards higher frequencies (average shift = +0.11 c/d, $p < 0.001$, Wilcoxon test). Those with

intermediate optimal spatial frequencies (between 0.4 and 0.5 c/d) did not have significant peak shifts (average shift = -0.04 c/d, $p = 0.272$, Wilcoxon test). Similar unreported correlations between peak shift and optimal spatial frequency of the cell were found when we re-analyzed the thalamic and cortical data from previous studies (Figure 5, $r= 0.45$, $p < 0.002$ for Nolt et al., 2004; $r= 0.52$, $p < 0.001$ of Sceniak et al., 2002).

Discussion

We have demonstrated that increasing stimulus contrast not only makes spatial frequency tuning of individual geniculate cells broader, but also generates a shift in their spatial frequency peaks. And these contrast-dependent peak shifts are not random but significantly correlated with the optimal spatial frequencies of these cells at high contrast. These results indicate that increasing the contrast not only broadens the spatial frequency tuning at the level of single neurons (by making each tuning wider), but also at the level of neuronal populations (by shifting the peak of the spatial frequency tuning in different directions depending on the spatial frequency peak of the cell), as illustrated by the cartoon shown in Figure 6.

Contrast-dependent spatial summation was first demonstrated in primary visual cortex (Kapadia et al., 1999; Sceniak et al., 1999; Cavanaugh et al., 2002) and it has been assumed that cortical networks are exclusively responsible for the expansion of the receptive field at low contrasts. For example, one hypothesis is that this property might involve changes of excitatory coupling between cortical cells (Sceniak et al., 1999). Under conditions of low contrast stimulation, lateral excitatory connections between cortical neurons with spatially nonoverlapping receptive fields are strong. This lateral coupling enhances spatial pooling of their receptive fields and increases the effective size of the central receptive field. As the input signal increases, lateral connections are weakened and spatial pooling is similarly reduced. Recent studies in the LGN suggested that the thalamic inputs to the visual cortex may also contribute to this contrast-dependent spatial property (Solomon et al., 2002; Nolt et al., 2004). The mean ratio of receptive field size at low contrast to that at high contrast is 1.31 in marmoset LGN (Solomon et

al., 2002) and 1.75 in cat LGN (Nolt et al., 2004). However, this value is 2-4 in primate V1 (Kapadia et al., 1999; Sceniak et al., 1999; Cavanaugh et al., 2002). Therefore, a significant contribution from the LGN cannot be ruled out. Nolt et al. also suggested that this contrast-dependent spatial summation may first arise in the retinal ganglion cells and is transmitted passively through the LGN to visual cortex (Nolt et al., 2004). Traditionally, the spatial frequency selectivity has been thought to be independent of stimulus contrast (Movshon et al., 1978; Albrecht and Hamilton, 1982; Sclar and Freeman, 1982; Li and Creutzfeldt, 1984; Bradley et al., 1987; Skottun et al., 1987; Sclar et al., 1990). However, if the spatial summation is not contrast-independent, then other spatial properties of the receptive field are also supposed to change with spatial summation at different contrast levels.

To our knowledge, this paper is the first to report the broadening of spatial frequency tuning at levels of both individual cells and neuronal populations with contrast, although this phenomenon was buried in the data from previous studies (Sceniak et al., 2002; Nolt et al., 2004). The reason that this phenomenon was ignored in the past is because spatial frequency peaks at high contrast was usually compared with those at low contrast directly. Our results and reanalysis of data from previous studies (Sceniak et al., 2002; Nolt et al., 2004) have shown that the shift of optimal spatial frequency with contrast was positive for some cells and negative for others. Moreover, the sign of these shifts depended on the optimal spatial frequency of the cell. Due to the cancellation effect, on average there was no significant change of spatial frequency peak with contrast in our data and in primate V1 data from (Sceniak et al., 2002). However, cat LGN data from (Nolt et al., 2004) showed that the spatial frequency peak increase with contrast due

to the fact that most of those LGN cells had relatively high optimal spatial frequencies. Similarly as the contrast-dependent spatial summation, the broadening of spatial frequency with contrast at both levels of single neurons and whole population was both found in thalamus and cortex. Our findings should shed some light on the computational modeling of the cortical architecture.

Broadening of spatial frequency tuning at levels of both individual cells and neuronal populations with contrast may enhance the ability of the visual system to accommodate a larger spectrum of stimulus features and analyze the visual information more precisely. On the other hand, a weak signal generated by low-contrast stimulus requires the visual system to gather information from more extensive regions of visual space at cost of reduced spatial resolution (Kapadia et al., 1999; Sceniak et al., 1999; Sceniak et al., 2001; Solomon et al., 2002; Nolt et al., 2004). All these adaptive changes of spatial properties with contrast may allow the visual system to optimize performance under changing stimulus conditions.

References

Albrecht DG, Hamilton DB (1982) Striate cortex of monkey and cat: contrast response function. J Neurophysiol 48:217-237.

Bradley A, Skottun BC, Ohzawa I, Sclar G, Freeman RD (1987) Visual orientation and spatial frequency discrimination: a comparison of single neurons and behavior. J Neurophysiol 57:755-772.

Cavanaugh JR, Bair W, Movshon JA (2002) Nature and interaction of signals from the receptive field center and surround in macaque V1 neurons. J Neurophysiol 88:2530-2546.

Eckhorn R, Thomas U (1993) A new method for the insertion of multiple microprobes into neural and muscular tissue, including fiber electrodes, fine wires, needles and microsensors. J Neurosci Methods 49:175-179.

Enroth-Cugell C, Robson JG (1966) The contrast sencitivity of retinal ganglion cells of the cat. J Physiol London 187:517-552.

Heeger DJ (1992) Normalization of cell responses in cat striate cortex. Vis Neurosci 9:181-197.

Hochstein S, Shapley RM (1976) Quantitative analysis of retinal ganglion cell classifications. J Physiol 262:237-264.

Jin JZ, Weng C, Yeh CI, Alonso JM (2004) Influence of contrast on the spatial properties of cells in the cat lateral geniculate nucleus. Abstract Viewer and Itinerary Planner Washington, DC: Society for Neuroscience, 2004 CD-ROM Program NO. 409.1.

Kapadia MK, Westheimer G, Gilbert CD (1999) Dynamics of spatial summation in primary visual cortex of alert monkeys. Proc Natl Acad Sci U S A 96:12073-12078.

Li CY, Creutzfeldt O (1984) The representation of contrast and other stimulus parameters by single neurons in area 17 of the cat. Pflugers Arch 401:304-314.

Movshon JA, Thompson ID, Tolhurst DJ (1978) Spatial and temporal contrast sensitivity of neurones in areas 17 and 18 of the cat's visual cortex. J Physiol 283:101-120.

Nolt MJ, Kumbhani RD, Palmer LA (2004) Contrast-dependent spatial summation in the lateral geniculate nucleus and retina of the cat. J Neurophysiol 92:1708-1717.

Ohzawa I, Sclar G, Freeman RD (1985) Contrast gain control in the cat's visual system. J Neurophysiol 54:651-667.

Pettigrew JD, Cooper ML, Blasdel GG (1979) Improved use of tapetal reflection for eye-position monitoring. Invest Ophthalmol Vis Sci 18:490-495.

Sceniak MP, Hawken MJ, Shapley R (2001) Visual spatial characterization of macaque V1 neurons. J Neurophysiol 85:1873-1887.

Sceniak MP, Hawken MJ, Shapley R (2002) Contrast-dependent changes in spatial frequency tuning of macaque V1 neurons: effects of a changing receptive field size. J Neurophysiol 88:1363-1373.

Sceniak MP, Ringach DL, Hawken MJ, Shapley R (1999) Contrast's effect on spatial summation by macaque V1 neurons. Nat Neurosci 2:733-739.

Sclar G, Freeman RD (1982) Orientation selectivity in the cat's striate cortex is invariant with stimulus contrast. Exp Brain Res 46:457-461.

Sclar G, Maunsell JH, Lennie P (1990) Coding of image contrast in central visual pathways of the macaque monkey. Vision Res 30:1-10.

Shapley R, Hochstein S (1975) Visual spatial summation in two classes of geniculate cells. Nature 256:411-413.

Skottun BC, Bradley A, Sclar G, Ohzawa I, Freeman RD (1987) The effects of contrast on visual orientation and spatial frequency discrimination: a comparison of single cells and behavior. J Neurophysiol 57:773-786.

So YT, Shapley R (1979) Spatial properties of X and Y cells in the lateral geniculate nucleus of the cat and conduction veolcities of their inputs. Exp Brain Res 36:533-550.

Solomon SG, White AJ, Martin PR (2002) Extraclassical receptive field properties of parvocellular, magnocellular, and koniocellular cells in the primate lateral geniculate nucleus. J Neurosci 22:338-349.

Weng C, Jin JZ, Yeh CI, Alonso JM (2007) Influence of contrast on the spatial frequency tuning of neuronal populations in the cat visual thalamus. Abstract Viewer and Itinerary Planner Washington, DC: Society for Neuroscience, 2007 CD-ROM Program NO. 392.29.

Yeh CI, Stoelzel CR, Alonso JM (2003) Two different types of Y cells in the cat lateral geniculate nucleus. J Neurophysiol 90:1852-1864.

Figure Legend

Figure 1. Receptive fields and spatial frequency tuning curves of 7 simultaneously recorded geniculate cells. The receptive fields are shown at the center (on-center cell: solid line; off-center cell: dashed line) and the spatial frequency tuning curves (fitted with Gaussian function) at the periphery (high contrast: continuous red line; low contrast: dashed blue line). The SF-Peak was defined as the spatial frequency elicited the maximum response. The SF-Bandwidth was calculated as the log ratio in octaves ($\log_2$ (SF-High cutoff/SF-Peak)), where SF-High cutoff was the spatial frequency that produced half of the maximum response on the right side of the Gaussian curve. As the stimulus contrast increased, the SF-Bandwidth became broader and the SF-peak shifted toward lower (Cells 1~4) or higher (Cells 6~7) spatial frequencies. The position of multi-electrode is shown at the upper left corner (AC: area centralis). Each geniculate cell is numbered from 1 to 7.

Figure 2. Spatial frequency bandwidths for all the LGN cells at two different contrasts. (A) Measurements of SF-Bandwidth with high (98%) and low (22%) contrast stimuli (X cell: light blue circle; Y cell: orange circle). The SF-Bandwidth was 41% broader at high contrast than at low contrasts ($p < 0.001$, Wilcoxon test). The insets show two examples. (B and C) The average bandwidth ratios for X cells (1.40) and Y cells (1.43) were not significantly different ($p > 0.05$, Wilcoxon test).

Figure 3. Spatial frequency peaks for all the LGN cells at two different contrasts. (A) Measurements of SF-Peak with high and low contrast stimuli (X cell: light blue circle; Y

cell: orange circle). There was no significant difference between the SF-Peaks at high and low contrasts ($p > 0.05$, Wilcoxon test). The insets show two examples. (B and C) The distribution of SF-Peak ratio (high-contrast/low-contrast) was similar for X and Y cells. The average SF-peak ratio for X cells (0.95) and Y cells (1.04) were not significantly different ($p > 0.05$, Wilcoxon test).

Figure 4. Changes in stimulus contrast produced a shift in SF-Peak in individual cells. (A) The shift of SF-Peak significantly correlated with SF-Peak measured at high contrast (X cells: $r = 0.72$, $p < 0.001$; Y cells: $r = 0.43$, $p < 0.001$). (B) Spatial frequency tuning curves obtained by making groups of LGN cells based on their SF-Peaks and then averaging all the cells within each group. The tuning curves shifted towards the left in cells with low values of SF-Peak (< 0.4 cycles/deg) and towards the right in cells with high values of SF-Peak (> 0.5 cycles/deg). These shifts in SF-Peak were significant for all groups except the group with SF-Peak between 0.4 and 0.5 cycles/deg (the significance values are illustrated by the number of asterisks as indicated at the bottom of the figure).

Figure 5. Unreported correlations between the shift of SF-Peak with contrast and SF-Peak measured at high contrast in previous studies. (A) LGN data adapted from Nolt et al. 2004, $r = 0.45$, $p < 0.002$; (B) Cortex data adapted from Sceniak et al. 2002, $r = 0.52$, $p < 0.001$.

Figure 6. Cartoon showing the influence of contrast at the spatial frequency tuning of geniculate cell population. The solid red lines represent spatial frequency tuning curves at high contrast and the blue dashed lines for low contrast. The lower part shows three representative cells with low, medium and high SF-peaks. Increasing the contrast broadens the spatial frequency tuning for each cell and generates different shifts for these three cells: negative shift for cell with low SF-peak, zero shift for cell with medium SF-peak, positive shift for cell with high SF-peak. The summed curves (upper part) show that increasing the contrast broadens spatial frequency tuning of neuronal population with relatively no change in SF-peak.

Figure 1

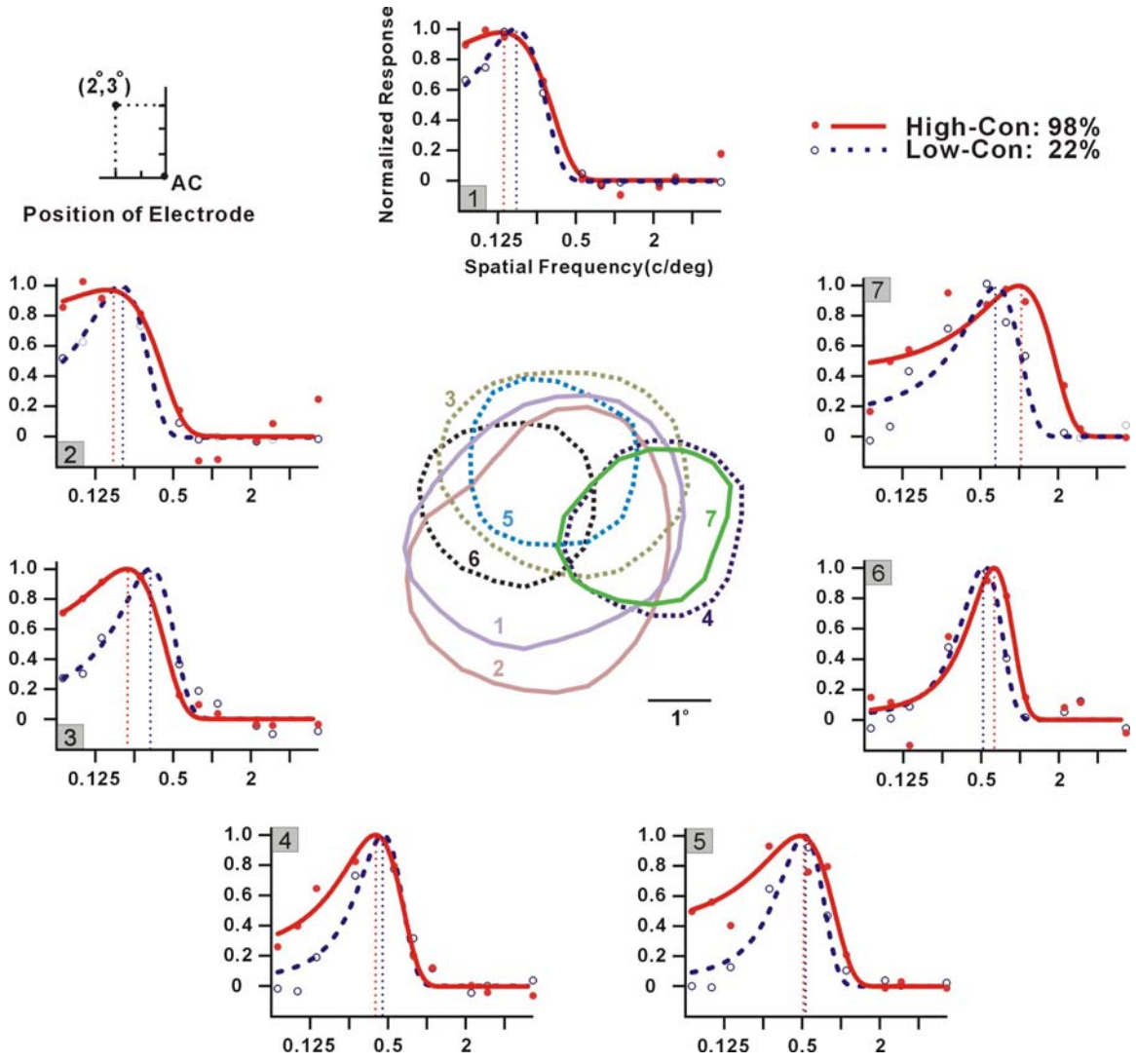
(2°,3°)
AC
Position of Electrode
Normalized Response
Spatial Frequency(c/deg)
High-Con: 98%
Low-Con: 22%
1°

Figure 2

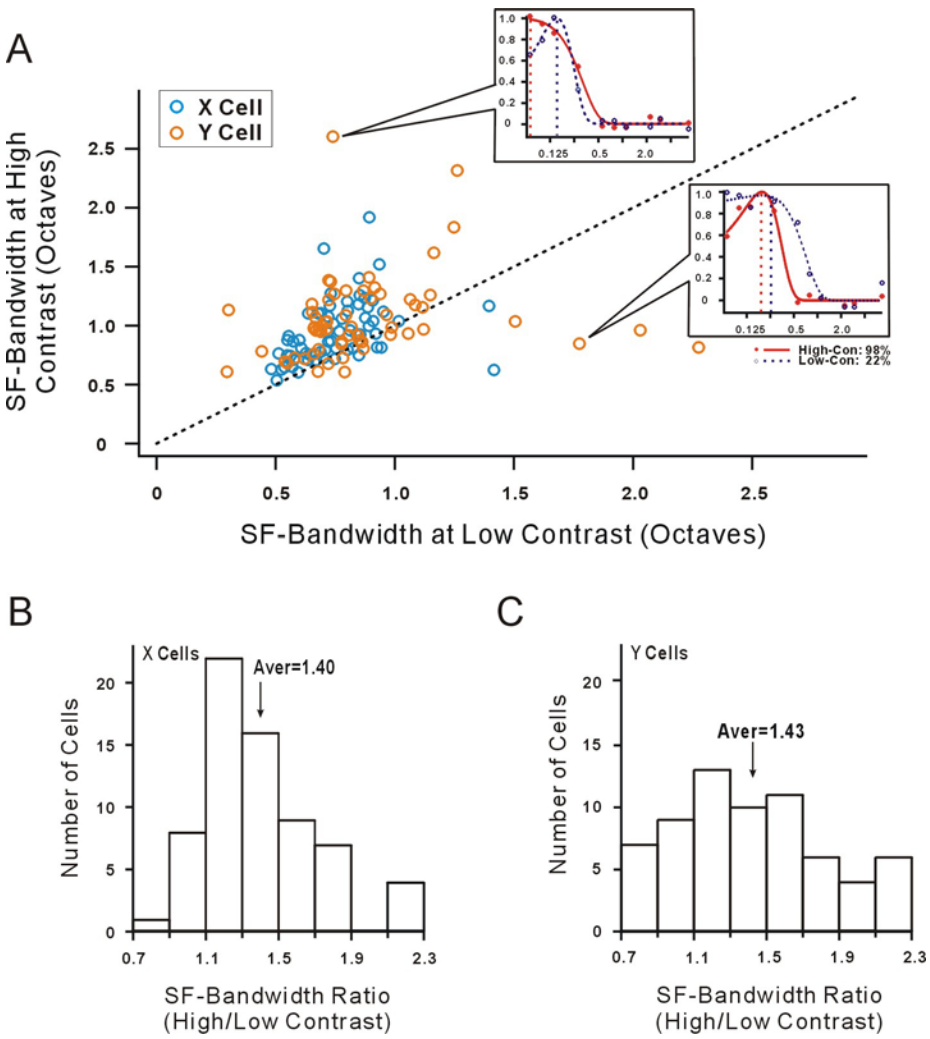
A
X Cell
Y Cell
SF-Bandwidth at High Contrast (Octaves)
SF-Bandwidth at Low Contrast (Octaves)
High-Con: 98%
Low-Con: 22%
B
X Cells
Aver=1.40
Number of Cells
SF-Bandwidth Ratio (High/Low Contrast)
C
Y Cells
Aver=1.43
Number of Cells
SF-Bandwidth Ratio (High/Low Contrast)

Figure 3

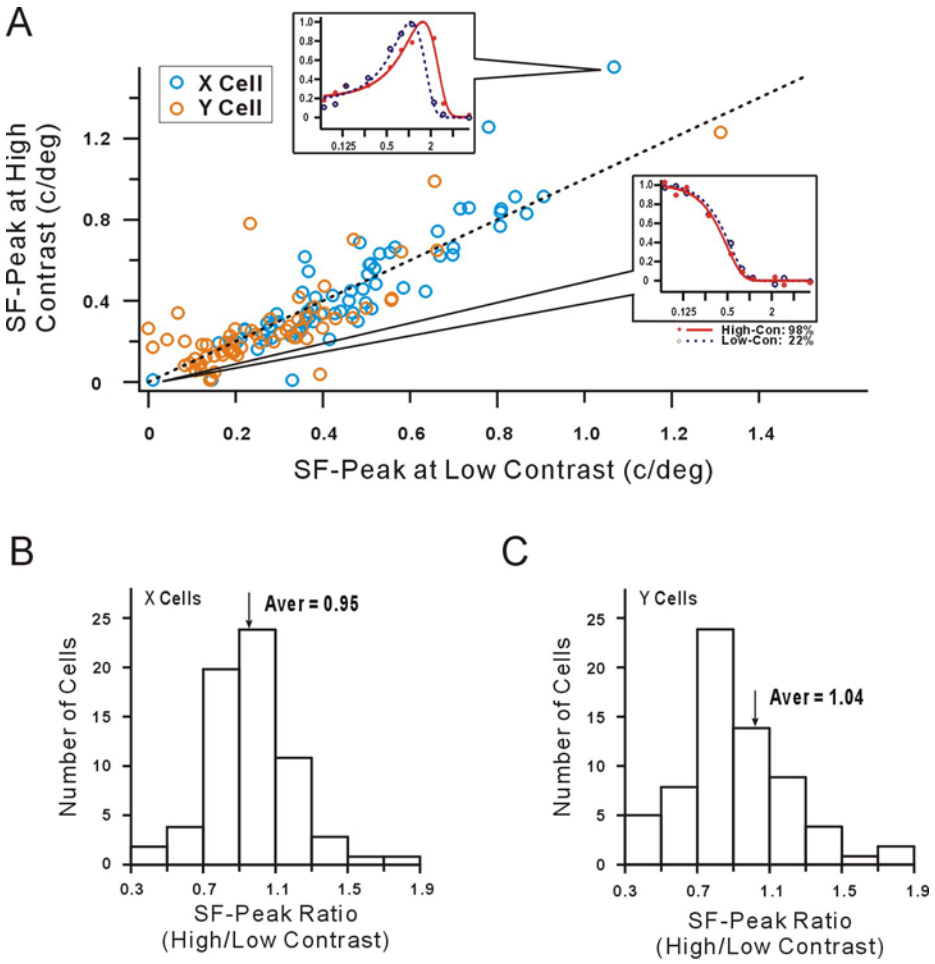
A
X Cell
Y Cell
SF-Peak at High Contrast (c/deg)
SF-Peak at Low Contrast (c/deg)
High-Con: 98%
Low-Con: 22%
B
X Cells
Aver = 0.95
Number of Cells
SF-Peak Ratio (High/Low Contrast)
C
Y Cells
Aver = 1.04
Number of Cells
SF-Peak Ratio (High/Low Contrast)

Figure 4

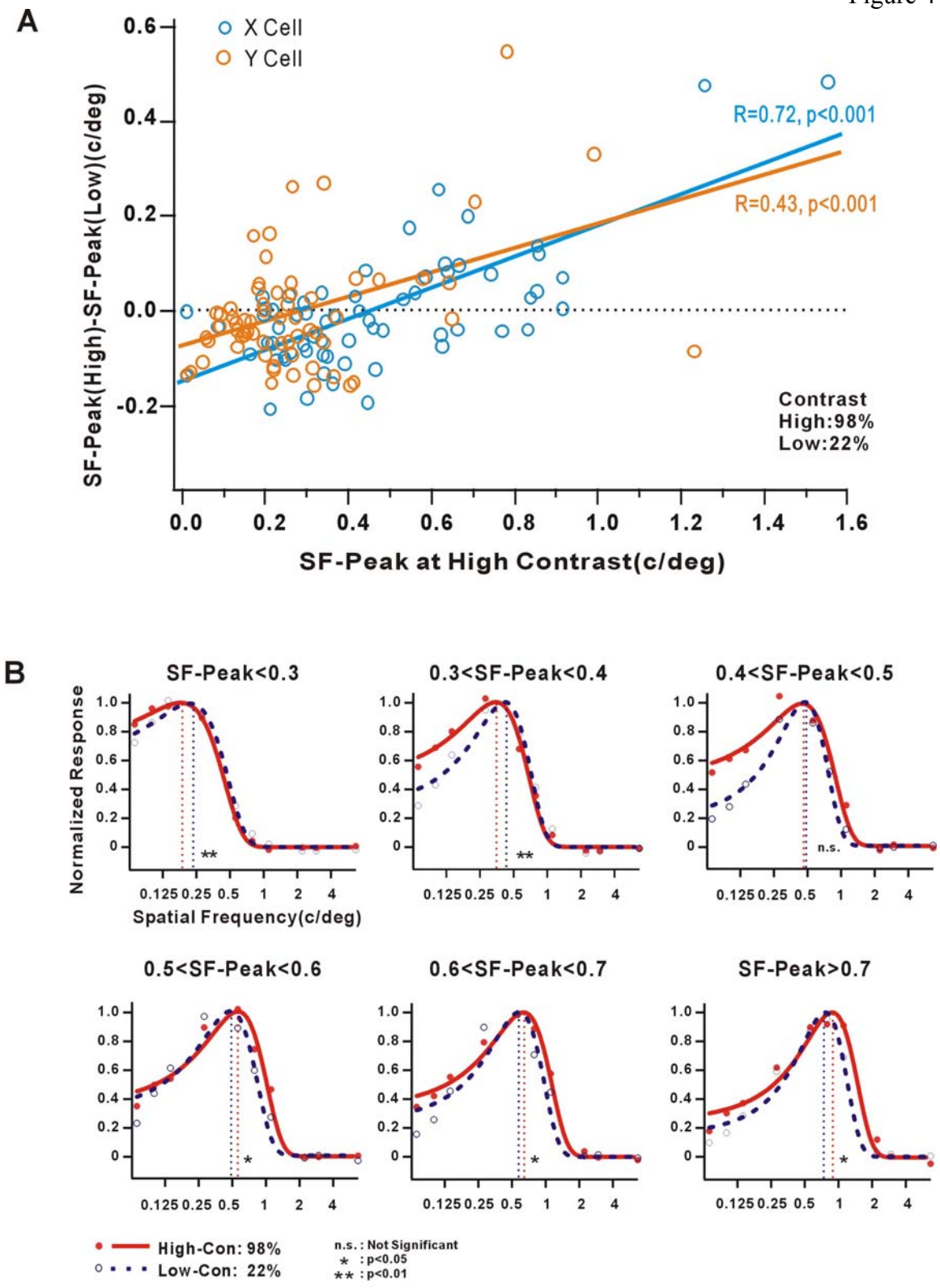
A
X Cell
Y Cell
R=0.72, p<0.001
R=0.43, p<0.001
Contrast
High:98%
Low:22%
SF-Peak(High)-SF-Peak(Low)(c/deg)
SF-Peak at High Contrast(c/deg)
B
SF-Peak<0.3
0.3<SF-Peak<0.4
0.4<SF-Peak<0.5
0.5<SF-Peak<0.6
0.6<SF-Peak<0.7
SF-Peak>0.7
Normalized Response
Spatial Frequency(c/deg)
High-Con: 98%
Low-Con: 22%
n.s. : Not Significant
* : p<0.05
** : p<0.01

Figure 5

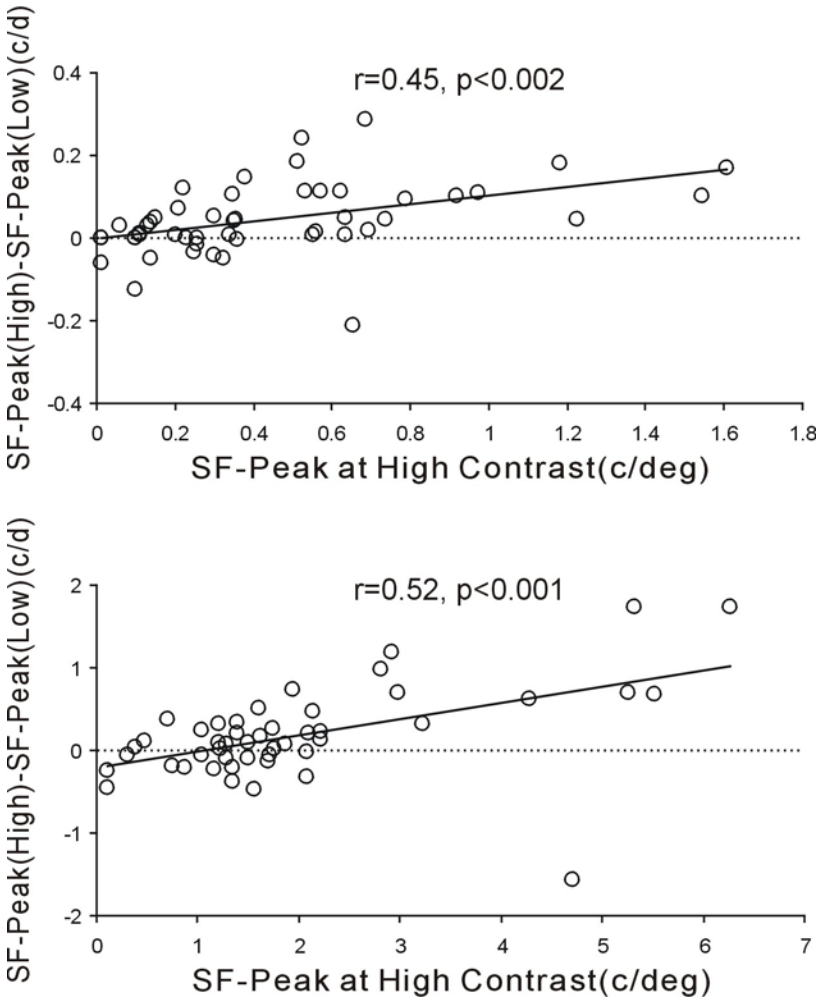
r=0.45, p<0.002
SF-Peak(High)-SF-Peak(Low)(c/d)
SF-Peak at High Contrast(c/deg)
r=0.52, p<0.001
SF-Peak(High)-SF-Peak(Low)(c/d)
SF-Peak at High Contrast(c/deg)

Figure 6

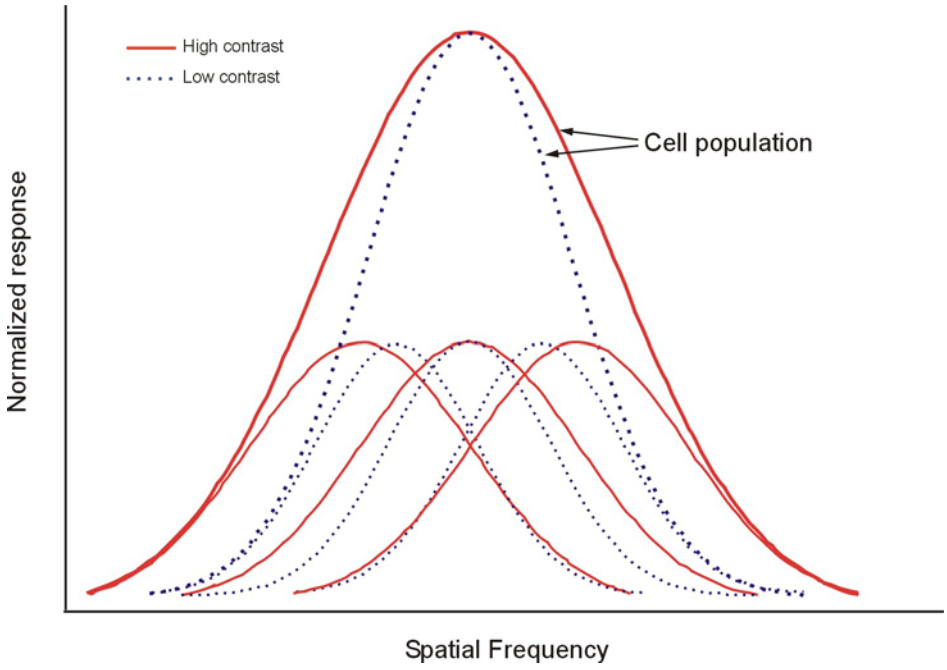
High contrast
Low contrast
Cell population
Normalized response
Spatial Frequency